# Supplementary Information

## Quasi-3D $Sb_2S_3$/Reduced Graphene Oxide/MXene ($Ti_3C_2T_x$) Hybrid for High-rate and Durable Sodium-Ion Batteries

Pengxin Li, Rui Zang, Yuhan Wu, Shuaishuai Liu, Siyu Wang, Puyu Liu, Peng Li*

College of Material Science and Engineering, Nanjing University of Aeronautics and Astronautics, Nanjing 211106, China.

*Corresponding author. E-mail: LPeng@nuaa.edu.cn;

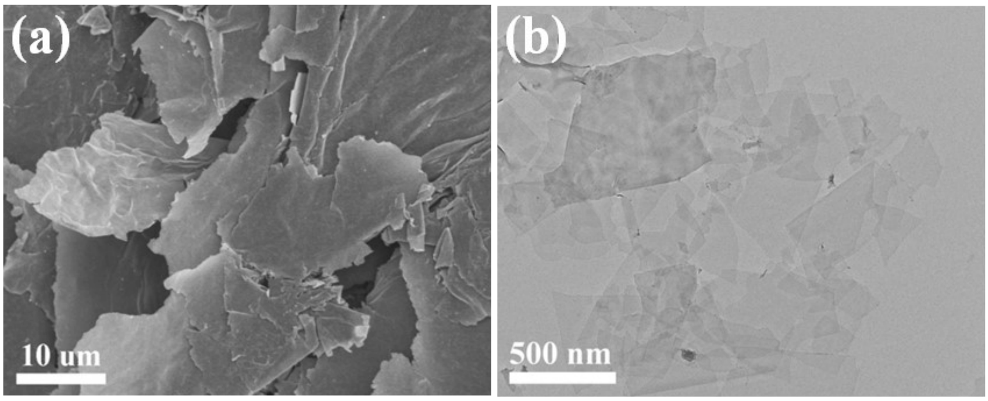


**Fig. S1** (a) SEM and (b) TEM images of the $Ti_3C_2T_x$ MXene.

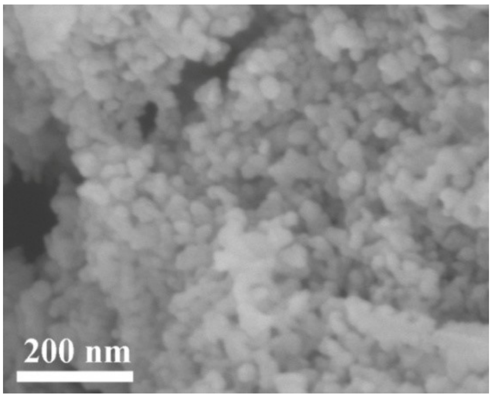


**Fig. S2** SEM image of the $Sb_2S_3$ nanoparticles.

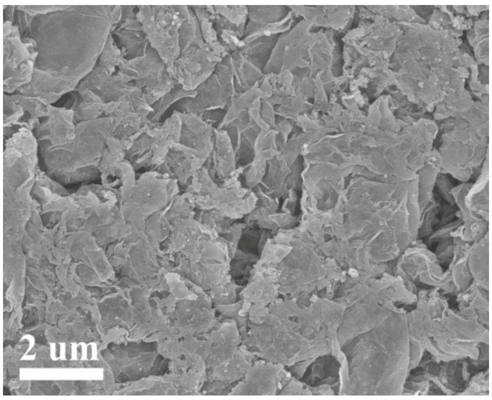


**Fig. S3** SEM image of the $Sb_2S_3$/RGO/MXene composite.

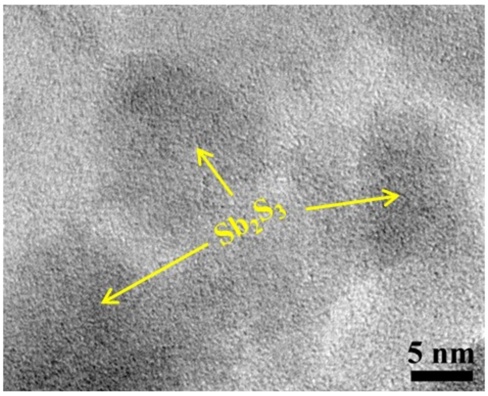


**Fig. S4** HRTEM image of the $Sb_2S_3$/RGO/MXene composite.

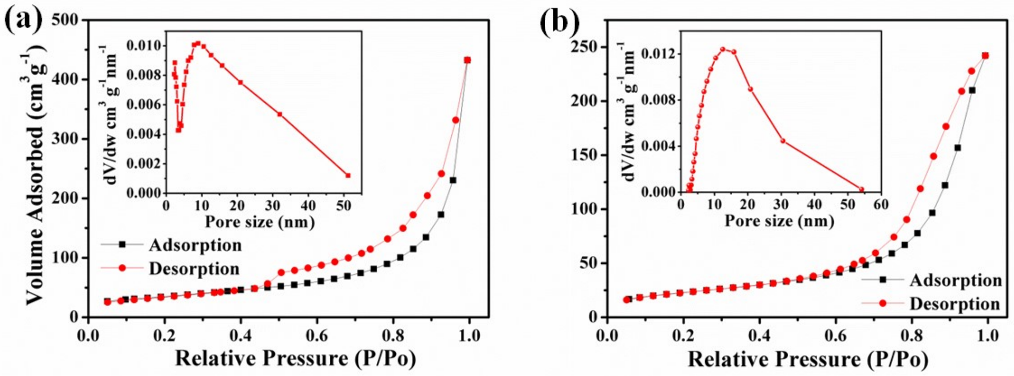


**Fig. S5** $N_2$ adsorption/desorption isotherms and the corresponding pore size distribution curve (inset) of the (a) $Sb_2S_3$/RGO and (b) $Sb_2S_3$/MXene composite.

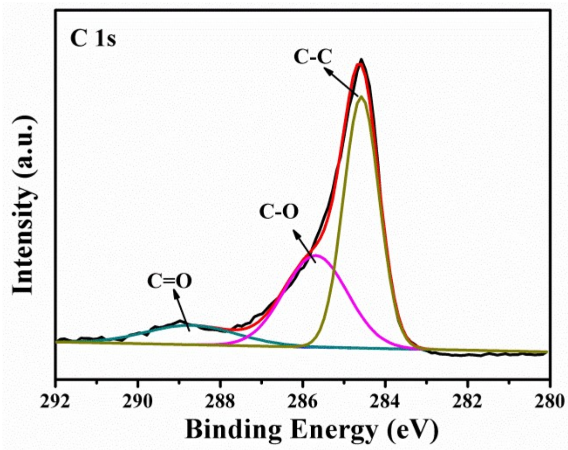


**Fig. S6** the high-resolution C 1s XPS spectra of $Sb_2S_3$/RGO composite

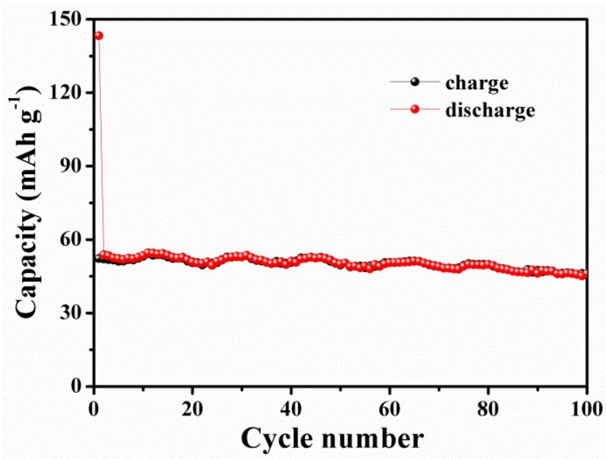


**Fig. S7** Cycling performances of the 3D RGO/MXene electrode

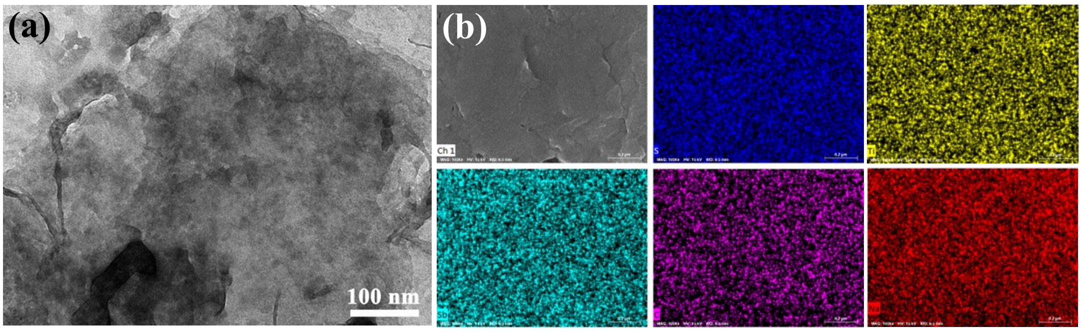


**Fig. S8** (a) TEM image of $Sb_2S_3$/RGO/MXene after 50 cycles at 0.2 $A \cdot g^{-1}$. (b) TEM elemental-mapping images for C, S, Sb, Ti and Na.

**Table S1** Electrochemical performance comparison between the $Sb_2S_3$/RGO/MXene composite and previously reported $Sb_2S_3$-based composites.

| Materials | Cycling stability (mAh $g^{-1}$) | Rate capability (mAh $g^{-1}$) |
|---|---|---|
| $Sb_2S_3$/CS[1] | 321 after 200 cycles at 0.2 A $g^{-1}$ | 221 at 5 A $g^{-1}$ |
| $Sb_2S_3$@MWCNTs[2] | 412.3 after 50 cycles at 0.05 A $g^{-1}$ | 399.1 at 1 A $g^{-1}$ |
| $Sb_2S_3$ nanorods@C[3] | 570 after 100 cycles at 0.1 A $g^{-1}$ | 337 at 2 A $g^{-1}$ |
| $Sb_2S_3$ hollow microspheres[4] | 384 after 50 cycles at 0.2 A $g^{-1}$ | 275 at 4 A $g^{-1}$ |
| $Sb_2S_3$/PPy Microspheres[5] | 427 after 50 cycles at 0.1 A $g^{-1}$ | 513 at 1 A $g^{-1}$ |
| amorphous $Sb_2S_3$ anoparticle[6] | 586 after 100 cycles at 0.05 A $g^{-1}$ | 534 at 3 A $g^{-1}$ |
| Sn@$Sb_2S_3$-rGO[7] | 541 after 70 cycles at 0.5 A $g^{-1}$ | 360 at 5 A $g^{-1}$ |
| $Sb_2S_3$/C[8] | 538 after 100 cycles at 0.2 A $g^{-1}$ | 520 at 2 A $g^{-1}$ |
| MWNTs@$Sb_2S_3$@PPy[9] | 500 after 85 cycles at 0.1 A $g^{-1}$ | 376 at 2 A $g^{-1}$ |
| **This work** | 633.3 after 100 cycles at 0.2 A $g^{-1}$<br>442.6 after 500 cycles at 2 A $g^{-1}$ | 510.1 at 4 A $g^{-1}$ |

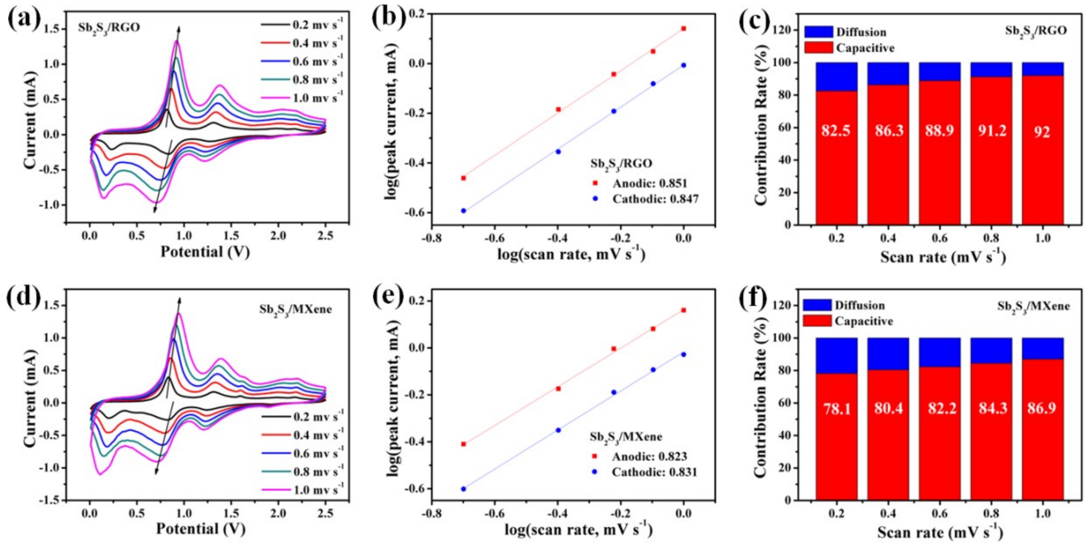


Fig. S9 (a, d) CV curves of the $Sb_2S_3$/RGO and $Sb_2S_3$/MXene electrode at different scan rates. (b, e) Corresponding log(i) versus log(v) plots for different redox peaks, respectively. (c, f) Capacitive contributions of the $Sb_2S_3$/RGO and $Sb_2S_3$/MXene electrode at various scan rates.

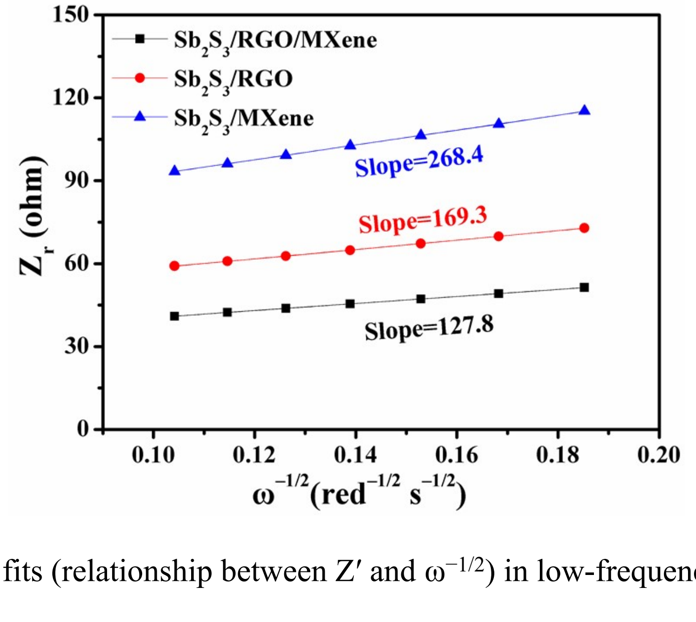


Fig. S10 Linear fits (relationship between $Z'$ and $\omega^{-1/2}$) in low-frequency region of the $Sb_2S_3$/RGO, $Sb_2S_3$/MXene and $Sb_2S_3$/RGO/MXene.

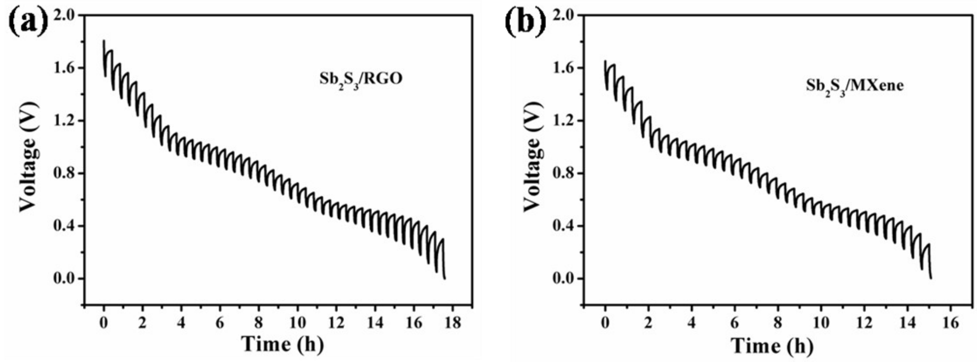


Fig. 11 The GITT curves of the $Sb_2S_3$/RGO and $Sb_2S_3$/MXene electrodes.

The value of $D_{GITT}$ can be calculated by applying the following equation:

$$D_{GITT} = \frac{4}{\pi\tau}\left(\frac{n\,Vm}{A}\right)^2\left(\frac{\Delta E_s}{\Delta E_\tau}\right)^2 \quad \left(\tau \ll \frac{L^2}{D}\right) \qquad \text{(S1)}$$

In equation S1, $\tau$ represents the pulse time; *n* is the amount of substance of the material, *Vm* is the molar volume of the material; *A* is the area of the electrode; *L* is the thickness of the electrode; $\Delta E_s$ is the voltage change caused by the pulse; $\Delta E_\tau$ represents the voltage change during the pulse.

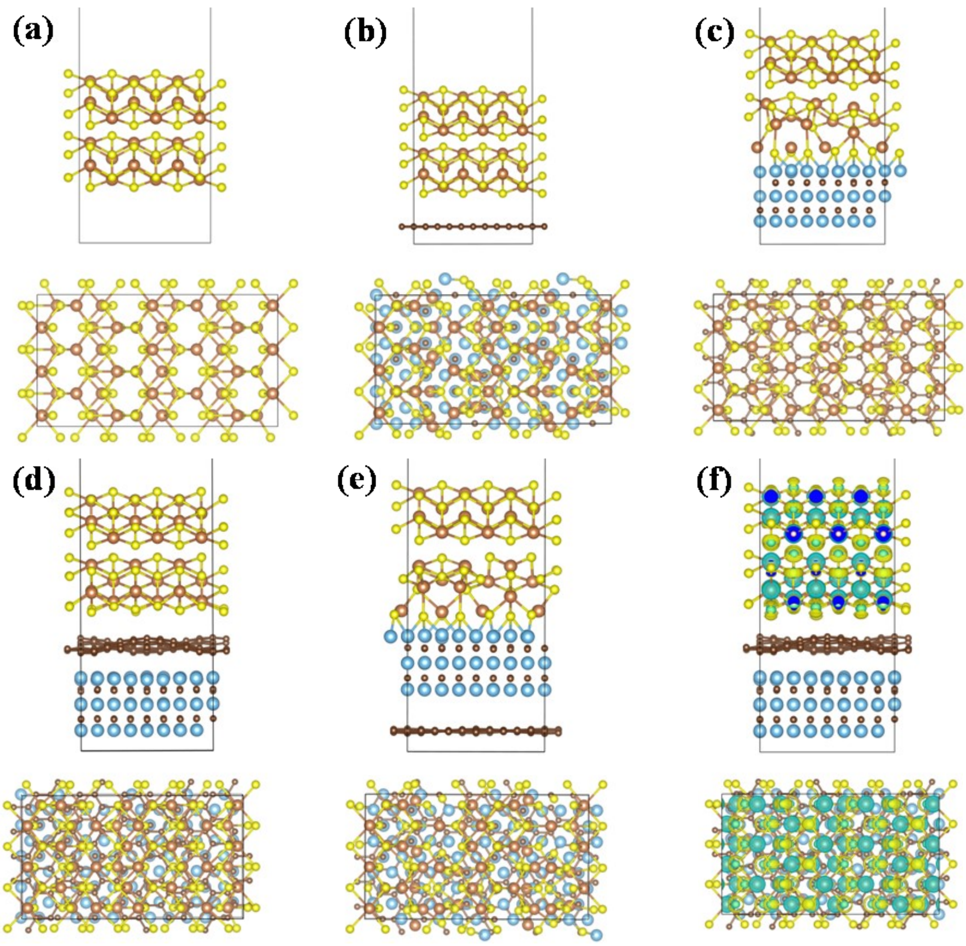


Fig. S12 Optimized structures for the adsorption of $Na^+$ on (a) $Sb_2S_3$, (b) $Sb_2S_3$/RGO, (c) $Sb_2S_3$/MXene, (d) $Sb_2S_3$-RGO-MXene and (e) $Sb_2S_3$-MXene-RGO at side (top) and top (bottom) views. (f) Differential charge density of the $Sb_2S_3$-RGO-MXene at side (top) and top (bottom) views.

Table S2 The adsorption energy of $Na^+$ on the $Sb_2S_3$, $Sb_2S_3$/RGO, $Sb_2S_3$/MXene and $Sb_2S_3$/RGO/MXene.

| | $Sb_2S_3$ | $Sb_2S_3$/RGO | $Sb_2S_3$/MXene | $Sb_2S_3$/RGO/MXene | |
|---|---|---|---|---|---|
| | | | | $Sb_2S_3$-RGO-MXene | $Sb_2S_3$-MXene-RGO |
| $E_{ads}$ | 1.38 eV | 1.36 eV | 1.40 eV | 1.35 eV | 1.49 eV |

## References


1. J. Xie, J. Xia, Y. Yuan, L. Liu, Y. Zhang, S. Nie, H. Yan and X. Wang, *J. Power Sources*, 2019, 435, 226762.
2. J. Li, Y. Dong, X. Zhang, S. Hu, D. Li, P. Likun, *Electrochimica Acta*, 2017, 228 ,436-446.
3. S. Yao, J. Cui, Z. Lu, Z. Xu, L.Qin, J. Huang, Z. Sadighi, F. Ciucci and J. K. Kim, *Adv. Energy Mater.*, 2017, 7, 1602149.
4. Y. Zhang, M. Li, Y. Ouyang, S. Nie and X. Wang, *Nano-Micro Letters*, 2018, 10, 12.
5. T. Zheng, G. Li, L. Zhao and Y. Shen, *Eur. J. Inorg. Chem.*, 2018, 10, 1224-1228.
6. S. Hwang, J. Kim and Y. Kim, *J. Mater. Chem. A*, 2016, 4, 17946-17951.
7. B. Qu, P. Deng, J. Yang, W. He and D. Tang, *ChemElectroChem*, 2018, 5, 1-7.
8. J. Choi, C. Ha, H. Choi, He. Shin and S. Lee, *Met. Mater. Int.*, 2017, 23, 1241-1249.
9. S. Wang，S. Yuan，Y. Yin，Y. Zhu，X. Zhang and J. Yan, *Part. Part. Syst. Char.*, 2016, 33, 493-499.